3J5-2

Proceedings of Symposium on Ultrasonic Electronics, Vol. 34 (2013) pp. 393-394
20-22 November, 2013

Monitoring of High-Intensity Focused Ultrasound Lesion Formation Using Decorrelation Between High-Speed Ultrasonic Images by Parallel Beamforming
平面波送信による超音波画像の非相関を用いた強力集束超音波の組織凝固モニタリング

Shoya Sasaki‡, Ryo Takagi, Keiko Matsuura, Shin Yoshizawa, and Shin-ichiro Umemura (Tohoku Univ.)
佐々木翔也‡, 高木亮, 松浦景子,吉澤晋, 梅村晋一郎 (東北大学)

1. Introduction

High-Intensity Focused Ultrasound (HIFU) is therapeutic treatment in which ultrasound is focused to a target tissue such as cancer to be thermally coagulated. In order to enhance the safety and accuracy of HIFU treatment, a noninvasive method to monitor thermal lesion formation is as important as a HIFU technology itself.

MRI and ultrasonic imaging are currently used for monitoring HIFU treatment. MRI has the advantage in tissue temperature measurement, but it lacks real-time monitoring capability. Ultrasonic imaging is chosen in this study because of its higher spatial and temporal resolution at much lower cost.

In this study, ultrasound 2D RF signals during HIFU exposure were acquired using high-speed imaging by parallel beamforming, and compared to estimate tissue coagulation. The distribution of cross-correlation coefficient between image blocks was calculated, where the tissue motion was compensated by a block matching algorithm. [1]

2. Material and Mathods

2.1 HIFU exposure and data acquisition

A freshly excised porcine liver was perfused with degassed saline to eliminate remaining gas and dissected to samples, and a sample was set in a tank containing degassed water as shown in **Fig. 1**. HIFU was generated from a focused transducer with a focal length of 70 mm at a driving frequency of 1.14 MHz. HIFU intensity was set to 1500 W/cm^2.

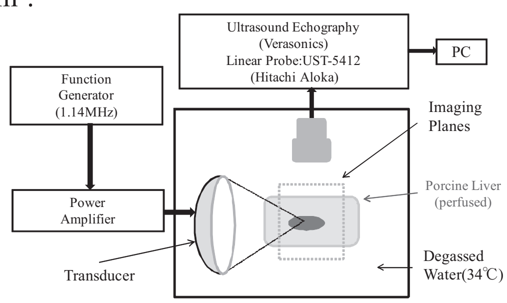

Fig. 1 Schematic of experimental setup

----

shoya.s@ecei.tohoku.ac.jp

The sequence of HIFU exposure and RF data acquisition is shown in **Fig. 2**.

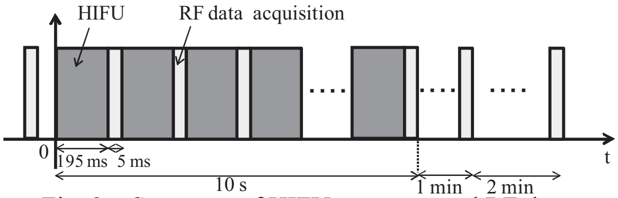

Fig. 2 Sequence of HIFU exposure and RF data acquisition

2.2 Ultrasound imaging

An ultrasound imaging system (Verasonics Inc.) and linear array probe (UST-5412,Aloka) were used for monitoring. The imaging plane was set so that it contains the axis of HIFU.

In normal ultrasound imaging, the focused ultrasound beams are transmitted a number of times to form a 2D image. However, in this study, we applied plane wave transmission followed by parallel beamforming for high-speed ultrasonic imaging. [2] To recover image contrast, multiple steered plane waves are transmitted (-18-18 degrees), and the obtained ultrasonic images are compounded.

2.3 Data analysis

To estimate the tissue coagulation, the cross-correlation coefficient was calculated between image blocks in each of the RF frames. Block matching was used for compensating tissue motion at the same time. First, a reference block was chosen in the reference frame, and then a block matching best to the reference block was searched in the target frame as shown in **Fig. 3**. Matching between the blocks was evaluated by a cross-correlation coefficient, calculated as

$$R = \frac{\sum_{i=1}^{M}\sum_{j=1}^{N} T(i,j) I^{*}(i,j)}{\sqrt{\sum_{i=1}^{M}\sum_{j=1}^{N} \left|T(i,j)\right|^{2}}\sqrt{\sum_{i=1}^{M}\sum_{j=1}^{N} \left|I(i,j)\right|^{2}}} \quad . (1)$$

Plotting the maximum value of the correlation coefficient as a function of the reference block position, a motion compensated distribution of correlation between the entire images can be depicted.

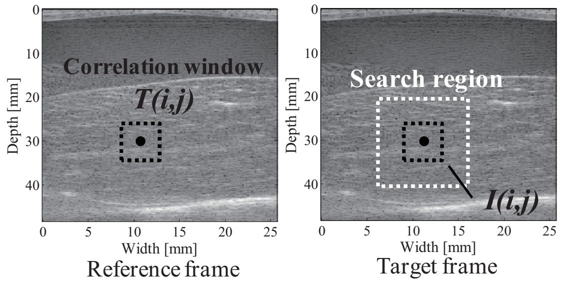

Fig. 3 Block matching based on cross-correlation coefficient

3. Result and Discussion

The distributions of cross-correlation coefficient at several times after the start of the sequence are shown in **Fig. 4**. The correlation coefficients were calculated between adjacent frames. Low correlation at the upper part of the distributions (less than about 10 mm in depth) is due to the water between the probe and the tissue. No change in the correlation is seen at 5.4 s, low correlation (about 0.9) is obeserved at 6.6 s at the central region corresponding to the focal spot of HIFU exposure, and an oval ring-shaped region of low correlation is seen at 8.4 s. These results suggest that ultrasound RF signals were varied by tissue coagulation, which started at around 6.6 s and gradually expanded up to at least 8.4 s.

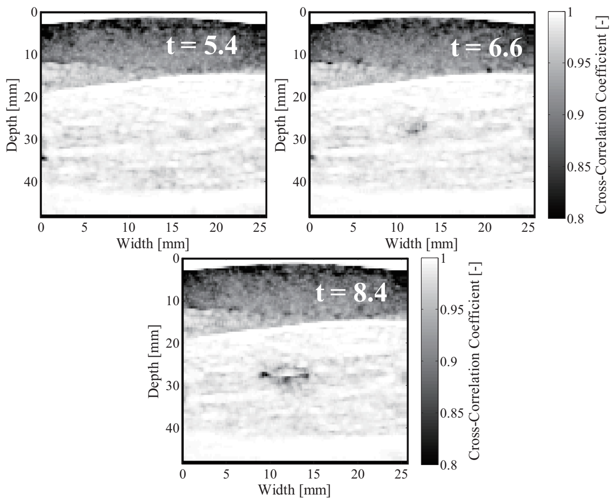

Fig. 4 Distributions of cross-correlation coefficient at several timings

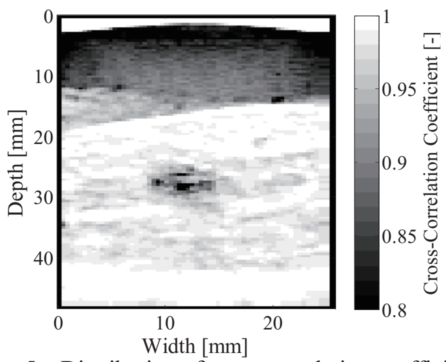

Fig. 5 Distribution of cross-correlation coefficient (minimum hold)

Minimum hold values of the cross-correlation coefficients between adjacent frames were calculated up to 10 s and mapped in **Fig. 5**. The size of decorrelated region measured by setting the threshold at 0.95 are 5.8 mm and 7.4 mm.

Fig. 6 shows the gross pathology of the tissue coagulation induced by HIFU exposure. The measured axial and lateral size of actual coagulation area were about 2.6 mm and 8.2 mm. The lateral size of the region of low correlation seen in Fig. 5 was approximately the same as the actual size of coagulation region, but the axial size was larger. This may be caused by the difference between the axial and lateral image resolution.

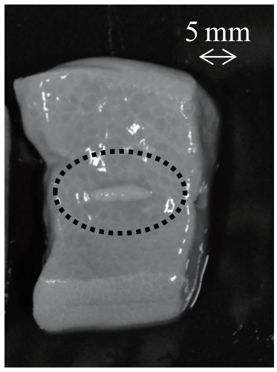

Fig. 6 Slice of sample after HIFU exposure

4. Conclusion

In this study, ultrasound 2D RF signals during HIFU exposure were compared by caluculating cross-correlation coefficient. The results show that decreased correlation was observed in the focal spot of HIFU exposure, and the progress of tissue coagulation could be seen by high-speed ultrasonic images by parallel beamforming. The proposed method may have the capability of real-time monitoring of HIFU lesion formation.

Acknowledgements

The auther would like to express their sincere thanks to Mr. S. Tamano of Hitachi Aloka Medical and Dr. T. Azuma of Tokyo Univ. for their cooperation in constructing the ultrasound imaging setup.

References

1. R.Matsuzawa, T.Shishitani, S.Yoshizawa, S.Umemura: Jpn. J. Appl. Phys. **51** (2012) 07GF26

2. G. Montaldo, M. Tanter, J. Bercoff, N. Benech, and M. Fink: IEEE Trans. Ultrason., Ferroelectr. Freq. Control, vol. 56, no. 3, pp. 489–506, Mar. 2009.